Pacific Northwest
NATIONAL LABORATORY

PNNL-38539

Two-Dimensional Silk Crystal Films as Matrix Layer for High-Performance Microelectronics

September 2025

Shaui Zhang
Antonino Tumeo
Chenyang Shi
Ankur Limaye
Dhruv Gajaria

U.S. DEPARTMENT of ENERGY

Prepared for the U.S. Department of Energy
under Contract DE-AC05-76RL01830

PACIFIC NORTHWEST NATIONAL LABORATORY
operated by
BATTELLE
for the
UNITED STATES DEPARTMENT OF ENERGY
under Contract DE-AC05-76RL01830

Printed in the United States of America

Available to DOE and DOE contractors from
the Office of Scientific and Technical Information,
P.O. Box 62, Oak Ridge, TN 37831-0062
www.osti.gov
ph: (865) 576-8401
fox: (865) 576-5728
email: reports@osti.gov

Available to the public from the National Technical Information Service
5301 Shawnee Rd., Alexandria, VA 22312
ph: (800) 553-NTIS (6847)
or (703) 605-6000
email: info@ntis.gov
Online ordering: http://www.ntis.gov

PNNL-38539

Two-Dimensional Silk Crystal Films as Matrix Layer for High-Performance Microelectronics

September 2025

Shuai Zhang
Antonino Tumeo
Chenyang Shi
Ankur Limaye
Dhruv Gajaria

Prepared for
the U.S. Department of Energy
under Contract DE-AC05-76RL01830

Pacific Northwest National Laboratory
Richland, Washington 99354

Abstract

This study explores a bio-inspired approach for memristive devices by combining Keggin-type polyoxometalates (POMs)-$[SiW_{12}O_{40}]_4$ (POM-T) and $[PW_{12}O_{40}]_3$ (POM-P), with silk fibroin (SF) to create 2D SF–POM layers on highly ordered pyrolytic graphite (HOPG) as resistive switching layers for memristors. We propose that the ordered SF layer template 0D POMs facilitate the formation of conductive filaments, thereby enhancing the variability of the manufactured memristors. AFM analysis revealed that both SF and SF–POM layers shared similar morphologies, while SF–POM–T formed larger aggregates, likely due to the stronger acidity of POM-T, which probably caused SF to aggregate and alter its secondary structure. Scanning Kelvin probe microscopy (SKPM) revealed that POMs reduced the contact potential difference of HOPG, resulting in lower work functions. Compared to an SF device, the SF–POM–P device showed improved memristive behavior, with a larger current gap and good repeatability over multiple sweeps; whereas the SF–POM–T device did not exhibit memristor activity, likely due to acidity-induced disruption of the SF template's order and CF formation. More importantly, SF–POM–P devices also demonstrated programmable memristive states. Finally, combining simulation-driven memristor modeling, we showcase a co-design workflow for advancing bioinspired memristors through new materials design, synthesis, and device modeling and development.

Summary

We examined SF–POM resistive switching layers for bio-inspired memristors by leveraging facilitated CF formation through templated POMs. AFM showed that SF and SF–POM layers have similar in-plane morphologies, while SF–POM–T formed larger aggregates due to the stronger acidity of POM-T. SKPM measurements revealed work-function reductions for the assembled layers: SF ≈ 4.59 eV, SF–POM–P ≈ 4.27 eV, and SF–POM–T ≈ 4.00 eV. At the device level, I-V curves indicate that SF–POM–P demonstrated improved memristive performance, characterized by a larger current gap and good repeatability across sweeps, whereas SF–POM–T showed no memristive activity, likely due to the disruption of crystallinity by acidity. Notably, SF–POM–P devices exhibited programmable memristive states, evidenced by current jumps between 1 and 2 V, consistent with the redox versatility of POM clusters. These results suggest that co-assembling SF with POMs can tune energy barriers and enable tunable, programmable, energy-efficient memristors. POM-P delivered superior performance, while POM-T highlights the important role of the chemical environment in modulating the order of the resistive switching layers and CF formation. This work supports a co-design approach for bio-inspired low-energy electronics, driven by simulation modeling for device design. Future efforts will focus on optimizing POM selection, SF crystallinity, and interface engineering to maximize device yield and stability. This project addresses the basic research need for microelectronics to “flip the current paradigm: define innovative material, device, and architecture requirements driven by applications, algorithms, and software.”

Acknowledgments

This research was supported by the Physical and Computational Science Directorate Mission Seed Investment, under the Laboratory Directed Research and Development (LDRD) Program at Pacific Northwest National Laboratory (PNNL). PNNL is a multi-program national laboratory operated for the U.S. Department of Energy (DOE) by Battelle Memorial Institute under Contract No. DE-AC05-76RL01830.

Acronyms and Abbreviations

AFM: Atomic Force Microscopy
HOPG: Highly Ordered Pyrolytic Graphite
I-V: Current-Voltage
POM: Polyoxometalate
SF: Silk Fibroin
SF-POM-P: Silk Fibroin–Polyoxometalate–Phosphorus
SF-POM-T: Silk Fibroin–Polyoxometalate–Tungsten
SPICE: Simulation Program with Integrated Circuit Emphasis

Contents

Figures

Tables

No table of figures entries found.

1.0 Introduction

Dennard scaling suggests that as transistors shrink, their dimensions and supply voltage decrease together to maintain constant power density. However, this no longer applies around 90-nm technology because leakage currents and short-channel effects prevent voltage scaling, leading to increased power density. (Johnsson and Netzer 2016; Lu et al. 2022) Therefore, developing new materials to enhance the energy efficiency of transistors—achieving better performance without raising power consumption—is crucial for advancing semiconductor technologies. (Shi et al. 2021)

Biological systems exhibit remarkably low-energy mechanisms for information transmission and electric energy transformation, enabled by the hierarchical organization of multi-component biomacromolecules. (Noy, Artyukhin, and Misra 2009; Wei et al. 2022) Biological synaptic power consumption is ~ 10 fJ per synaptic event (Wang et al. 2023), much less than that of widely used inorganic transistors. Additionally, biological memristors have the advantages of non-volatile storage and fast processing speed. Drawing inspiration from biological synapses, bio-inspired memristors are attracting significant attention for their potential to revolutionize computing, energy-efficient electronics, and bio-integrated technologies, representing a paradigm in neuromorphic computing and microelectronics. (Kim et al. 2022; Shi, Heble, and Zhang 2024; Shi et al. 2020) However, one essential challenge of the bio-inspired memristors is the variability between devices and measurements. (Wang et al. 2023; Shi et al. 2020; Shi et al. 2021) Generally speaking, the operation and mechanism of memristors are controlled by the formation of conductive filaments (CFs) through resistive switching layers. (Kaniselvan et al. 2025; Mehonic et al. 2020) The efficient information transfer in bio-inspired memristors hinges on the reliable formation and dissolution of CFs, which are determined by crystallinity, defect density, and interfacial stability with electrodes. (Mehonic et al. 2020; Shi et al. 2021) Therefore, developing a biomimetic resistive switching layer with a controlled structure and associated CF formation is essential for improving biomemristors' performance.

Our recent work achieved a new 2D crystalline phase of silk fibroin (SF) self-assembled on graphite and MoS_2, exhibiting an epitaxial relationship with the underlying lattice. (Shi et al.) Additionally, this assembly reduces the surface potential of highly oriented pyrolytic graphite (HOPG), significantly lowering the barrier to metal ion migration during CF growth and increasing the transport rate of charged particles in protein films. (Shi et al. 2019; Shi et al.) In this seed LDRD, we developed a novel strategy using 2D silk crystal films to template zero-dimensional semiconducting nanoclusters, polyoxometalates (POMs) (Chen et al. 2018), through advanced molecular epitaxial growth at HOPG-liquid interfaces for bio-inspired memristors. We employed scanning Kelvin force microscopy (SKPM) to characterize the work function (WF) of the synthesized 2D layer and discovered that POMs effectively tune its work function to facilitate electron injections. Additionally, we fabricated memristors utilizing the silk-POM 2D layer as the resistive switching component and used I-V measurements to demonstrate improved stability, repeatability, and programmable memristive states. Finally, we used simulation-driven memristor modeling to explore the feasibility of the co-design workflow for SF-POM memristors. This seed project establishes a co-design methodology, initiates characterization, forms a collaborative team bridging new materials synthesis and device design, and offers a roadmap for the practical testing and prototyping of innovative microelectronics devices.

2.0 Project results

2.1 2D SF-POM layers

In this work, we selected two Keggin-type POMs, $[SiW_{12}O_{40}]^{4-}$ (POM-T) and $[PW_{12}O_{40}]^{3-}$ (POM-P), to synthesize 2D-SF-POM layers on HOPG. (Figure 1A) We combined a 10 mg/ml SF solution with a 1 mg/ml POM solution in water, then drop-cast the mixture onto a freshly cleaved HOPG surface (Figure 1B) and dried it. AFM images show that the SF and SF-POM-P layers have similar morphologies (Figure 1C and 1E), while the SF-POM-T layer contains some large aggregates (indicated by the arrow in Figure 1D). Both POM-T and POM-P are 0D nanoclusters smaller than 1 nm in diameter. However, POM-T is more acidic than POM-P. AFM measurements suggest that, although the small size of POMs allows for good distribution within the SF layer without disrupting in-plane order and morphology, the acidic conditions caused by POM-T (pH 1-2) may lead to SF aggregation and changes in secondary structure. Additionally, we used SKPM to measure the surface potentials of the synthesized SF-POM layers. Previous research showed that the standard SF layer can lower the contact potential difference (CPD) of HOPG by about 60 mV.(Shi et al.) Figure 1F shows that the presence of POMs further decreases the CPD by several hundred millivolts. Using the equation $\varphi_{sample} = \varphi_{tip} - e\cdot CPD$, where φ_{sample} and φ_{tip} are the work functions (WFs) of the sample and AFM tip, respectively, and considering the known WF of HOPG (4.65 eV), we calculated the WFs of the SF, SF-POM-P, and SF-POM-T layers as 4.59 eV, 4.27 eV, and 4.00 eV, respectively. Therefore, employing the co-assembled 2D SF-POMs as the resistive switching layer in memristors is expected to enhance electron injection and filament formation, as well as energy efficiency.

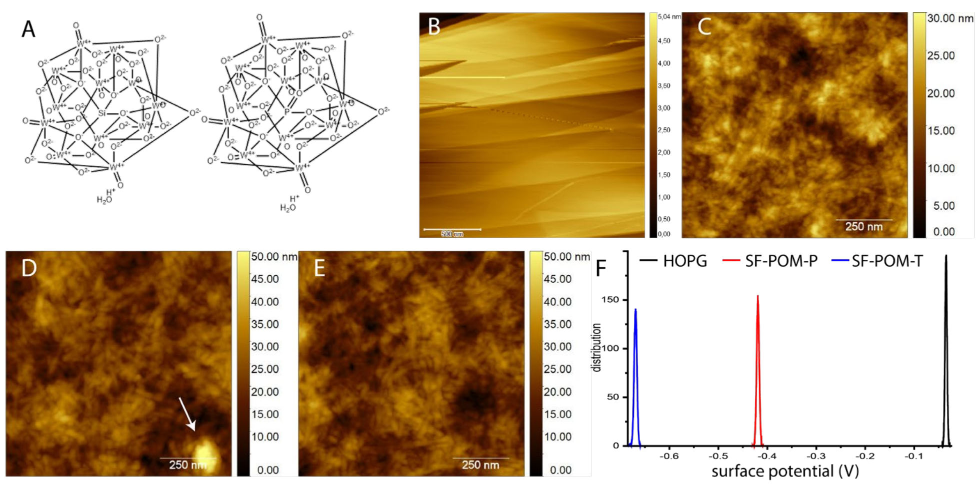

Figure 1. 2D SF-POM layers and characterizations. A) the structures of POM-T and POM-P. B-E) the AFM height images of bare HOPG, SF on HOPG, SF-POM-T on HOPG, and SF-POM-P on HOPG, respectively. F) the measured surface potential of HOPG, SF-POM-P, and SF-POM-T, respectively.

2.2 SF-POM memristors

We further used the SF and synthesized SF-POM as resistive switching layers to fabricate memristors in a vertical configuration (Figure 2A and 2B). Figure 3C shows the I-V measurement of a pure-SF memristor. It exhibits poor switching and memristive performance, with a small current gap between the opposite voltage sweep directions. In contrast, the SF-

POM-P device shows enhanced memristive performance with a larger current gap (Fig. 2D). Furthermore, the I-V curves demonstrate good repeatability after five consecutive sweeps. This suggests that the CF growth during the voltage sweep is facilitated by the POM-P clusters, due to the reduced WF and regulated electron migration. Encouragingly, the I-V curves of the SF-POM-P device display several current jumps between 1 V and 2 V (Figure 2E). These jumps indicate programmable memristive states, leveraging the programmable and reversible reduction-oxidation states of POM clusters (Moors and Monakhov 2024; Primera-Pedrozo et al. 2023). Therefore, the synthesized SF-POM-P 2D layers have promising applications in improving memristor variability, increasing information density, and enhancing energy efficiency through programmable memristor states. Lastly, the SF-POM-T device did not show any memristor performance (data not shown). One possible reason is that the acidic condition of POM-T, pH 1-2, decreases the structural homogeneity of the 2D-SF-POM-T layer (indicated by the arrow in Figure 1D) and disrupts the crystallinity and secondary structure of the SF template. Although the SF-POM-T layer has a lower WF than SF-POM-P, the device using SF-POM-T as the resistive switching layer performed poorly. This highlights the importance of co-designing when developing new memristors.

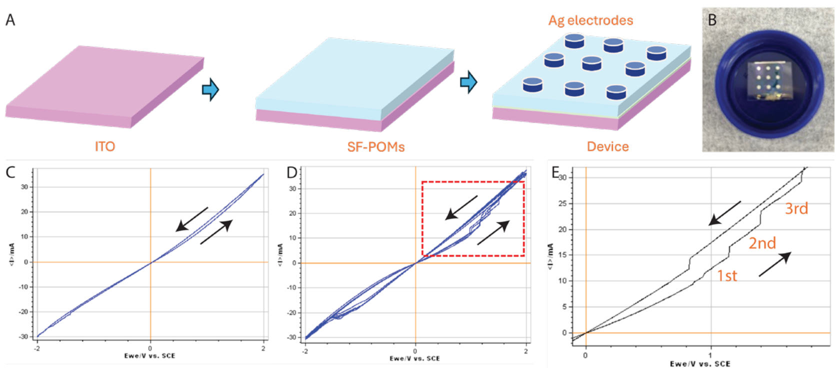

Figure 2. SF-POM-P device. A) the device configuration. B) the photo of a fabricated SF-POM device. C) I-V curve of pure Silk memristor. D) five consecutive swept I-V curves of the Silk-POM-P memristor. E) the zoom-in I-V curve from Panel D referring to various memristor states (1st-3rd). The arrows indicate the directions of the voltage sweeps.

2.3 Simulation-driven memristor modeling for device co-design

In parallel with the design and synthesis of SF-POM materials, as well as the associated device fabrication and testing, our team explores the feasibility of building a co-design framework for the SF-POM device using a simulation program with integrated circuit emphasis (SPICE) model to simulate the device. (Figure 3A) SPICE simulation can drive memristor co-design by giving materials scientists and device engineers a shared, actionable representation of a device, speeding up iteration between device discovery and circuit integration. (McAndrew et al. 2025; Li and Shi 2021) The simulation from the SPICE model will translate measured I-V hysteresis into a small set of parameter changes and run virtual experiments (sweep amplitude, frequency) that would be slow or costly in the lab. Additionally, device designers can plug the same model into driver, sense amplifier, and array simulations to test read/write margins, variability sensitivity, and failure modes before hardware is fabricated.

Our approach uses measured I–V data and design space exploration, with the Bouc–Wen model (Ismail, Ikhouane, and Rodellar 2009; Ikhouane, Mañosa, and Rodellar 2007) providing a mathematical foundation. The Bouc–Wen is a compact phenomenological model of hysteresis that uses a single internal state variable, which changes in response to the electrical stimulus. This variable, along with a simple conductance law, creates the characteristic I–V loops seen in many memristive devices, all with a small set of intuitive parameters—our SPICE. .subckt implementation exposes 14 adjustable parameters (k, alpha0, alphad, pshape, vscale, A, beta, gamma, n, Cdiff, zinit, zleak, zscale, and gfloor), some of which control the static I–V shape and pinching, while others govern the internal-state dynamics, affecting the loop width and rate effects.

The design space exploration employs a multi-stage Python pipeline that evaluates parameter sets based on their alignment with the I–V loop shape, timing, peak currents, and origin slope of experimental data. This step-by-step approach ensures the final parameter set is not only a good numerical fit but also reflects physically meaningful device behavior, making it robust for larger circuit simulations. The resulting SPICE model integrates seamlessly into standard simulation workflows and is especially suited for low-frequency or quasi-static experiments (seconds to minutes), where Bouc–Wen assumptions hold best. (Figure 3B) This demonstrates that the developed SPICE model can explore the design space of the SF-POM device to guide the development of SF-POM memristors, including material choices and device scales for a co-design workflow.

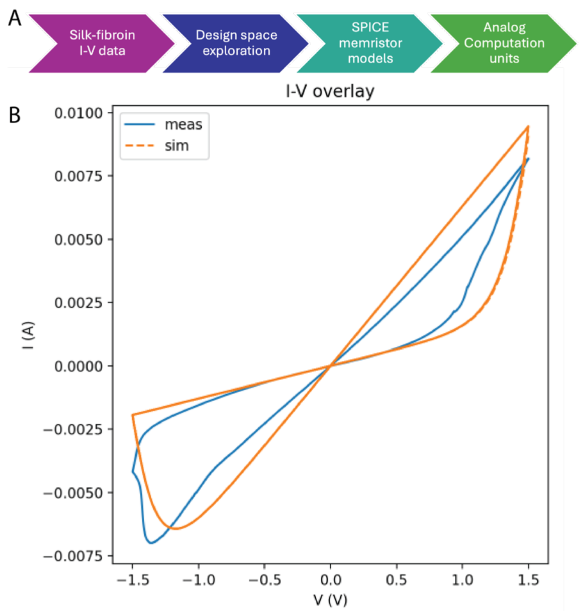

Figure 3. Simulation-driven memristor modeling. A) the workflow of the simulation-driven circuit design. B) the raw I-V curve of an SF memristor and the simulated IV-curve using the Bouc–Wen model.

3.0 References

Chen, Xiaoli, Jingyi Pan, Jingjing Fu, Xin Zhu, Chen Zhang, Li Zhou, Yan Wang, Ziyu Lv, Ye Zhou, and Su-Ting Han. 2018. "Polyoxometalates-Modulated Reduced Graphene Oxide Flash Memory with Ambipolar Trapping as Bidirectional Artificial Synapse." *Advanced Electronic Materials* 4 (12):1800444. doi: https://doi.org/10.1002/aelm.201800444.

Ikhouane, Fayçal, Víctor Mañosa, and José Rodellar. 2007. "Dynamic properties of the hysteretic Bouc-Wen model." *Systems & Control Letters* 56 (3):197-205. doi: https://doi.org/10.1016/j.sysconle.2006.09.001.

Ismail, Mohammed, Fayçal Ikhouane, and José Rodellar. 2009. "The Hysteresis Bouc-Wen Model, a Survey." *Archives of Computational Methods in Engineering* 16 (2):161-188. doi: 10.1007/s11831-009-9031-8.

Johnsson, L., and G. Netzer. 2016. "The impact of Moore's Law and loss of Dennard scaling: Are DSP SoCs an energy efficient alternative to x86 SoCs?" *Journal of Physics: Conference Series* 762 (1):012022. doi: 10.1088/1742-6596/762/1/012022.

Kaniselvan, M., Y. R. Jeon, M. Mladenović, M. Luisier, and D. Akinwande. 2025. "Mechanisms of resistive switching in two-dimensional monolayer and multilayer materials." *Nature Materials* 24 (9):1346-1358. doi: 10.1038/s41563-025-02170-5.

Kim, Kwan-Nyeong, Min-Jun Sung, Hea-Lim Park, and Tae-Woo Lee. 2022. "Organic Synaptic Transistors for Bio-Hybrid Neuromorphic Electronics." *Advanced Electronic Materials* 8 (1):2100935. doi: https://doi.org/10.1002/aelm.202100935.

Li, Bo, and Guoyong Shi. 2021. "A Native SPICE Implementation of Memristor Models for Simulation of Neuromorphic Analog Signal Processing Circuits." *ACM Trans. Des. Autom. Electron. Syst.* 27 (1):Article 6. doi: 10.1145/3474364.

Lu, Boyang, Lai Wang, Zhibiao Hao, Yi Luo, Chien-Ju Chen, Meng-Chyi Wu, Jianshi Tang, Jong Kyu Kim, and E. Fred Schubert. 2022. "Dennard Scaling in Optoelectronics: Scientific Challenges and Countermeasures of Micro-LEDs for Displays." *Laser & Photonics Reviews* 16 (12):2100433. doi: https://doi.org/10.1002/lpor.202100433.

McAndrew, C. C., A. J. Scholten, K. K. Gullapalli, Y. Chauhan, and K. Xia. 2025. "Benchmarks for SPICE Modeling and Parameter Extraction Based on AI/ML." *IEEE Transactions on Electron Devices* 72 (4):1551-1559. doi: 10.1109/TED.2025.3537952.

Mehonic, Adnan, Abu Sebastian, Bipin Rajendran, Osvaldo Simeone, Eleni Vasilaki, and Anthony J. Kenyon. 2020. "Memristors—From In-Memory Computing, Deep Learning Acceleration, and Spiking Neural Networks to the Future of Neuromorphic and Bio-Inspired Computing." *Advanced Intelligent Systems* 2 (11):2000085. doi: https://doi.org/10.1002/aisy.202000085.

Moors, Marco, and Kirill Yu Monakhov. 2024. "Capacitor or Memristor: Janus Behavior of Polyoxometalates." *ACS Applied Electronic Materials* 6 (12):8552-8557. doi: 10.1021/acsaelm.3c01751.

Noy, Aleksandr, Alexander B. Artyukhin, and Nipun Misra. 2009. "Bionanoelectronics with 1D materials." *Materials Today* 12 (9):22-31. doi: https://doi.org/10.1016/S1369-7021(09)70248-2.

Primera-Pedrozo, Oliva M., Shuai Tan, Difan Zhang, Brian T. O'Callahan, Wenjin Cao, Eric T. Baxter, Xue-Bin Wang, Patrick Z. El-Khoury, Venkateshkumar Prabhakaran, Vassiliki-Alexandra Glezakou, and Grant E. Johnson. 2023. "Influence of surface and intermolecular interactions on the properties of supported polyoxometalates." *Nanoscale* 15 (12):5786-5797. doi: 10.1039/D2NR06148A.

Shi, Chenyang, Annie Y. Heble, and Shuai Zhang. 2024. "Multiparametric AFM insights into electron transport mechanisms in biomemristors." *Materials Today Physics* 44:101429. doi: https://doi.org/10.1016/j.mtphys.2024.101429.

Shi, Chenyang, Fan Hu, Ronghui Wu, Zijie Xu, Guangwei Shao, Rui Yu, and Xiang Yang Liu. 2021. "New Silk Road: From Mesoscopic Reconstruction/Functionalization to Flexible Meso-Electronics/Photonics Based on Cocoon Silk Materials." *Advanced Materials* 33 (50):2005910. doi: https://doi.org/10.1002/adma.202005910.

Shi, Chenyang, Jinling Lan, Jingjuan Wang, Shuai Zhang, Youhui Lin, Shuihong Zhu, Amy E. Stegmann, Rui Yu, Xiaobing Yan, and Xiang Yang Liu. 2020. "Flexible and Insoluble Artificial Synapses Based on Chemical Cross-Linked Wool Keratin." *Advanced Functional Materials* 30 (45):2002882. doi: https://doi.org/10.1002/adfm.202002882.

Shi, Chenyang, Jingjuan Wang, Maria L Sushko, Wu Qiu, Xiaobing Yan, and Xiang Yang Liu. 2019. "Silk flexible electronics: from Bombyx mori silk Ag nanoclusters hybrid materials to mesoscopic memristors and synaptic emulators." *Advanced Functional Materials* 29 (42):1904777.

Shi, Chenyang, Marlo Zorman, Xiao Zhao, Miquel B. Salmeron, Jim Pfaendtner, Xiang Yang Liu, Shuai Zhang, and James J. De Yoreo. "Two-dimensional silk." *Science Advances* 10 (38):eado4142. doi: 10.1126/sciadv.ado4142.

Wang, Saisai, Rui Wang, Yaxiong Cao, Xiaohua Ma, Hong Wang, and Yue Hao. 2023. "Bio-Voltage Memristors: From Physical Mechanisms to Neuromorphic Interfaces." *Advanced Electronic Materials* 9 (4):2200972. doi: https://doi.org/10.1002/aelm.202200972.

Wei, Hao, Jiwei Min, Yuefei Wang, Yuhe Shen, Yaohui Du, Rongxin Su, and Wei Qi. 2022. "Bioinspired porphyrin–peptide supramolecular assemblies and their applications." *Journal of Materials Chemistry B* 10 (45):9334-9348. doi: 10.1039/D2TB01660E.

Pacific Northwest
National Laboratory

902 Battelle Boulevard
P.O. Box 999
Richland, WA 99354

1-888-375-PNNL (7665)

www.pnnl.gov